

MHD Buoyancy Flows of Cu, Al₂O₃ and TiO₂ nanofluid near Stagnation-point on a Vertical Plate with Heat Generation

Ifsana Karim¹, Md. Sirajul Islam², M.M. Rahman³, Md. Shakhaoath Khan^{1*}

¹ Department of Chemical Engineering, School of Engineering, University of Newcastle, Callaghan, NSW 2308, AUSTRALIA.

² Department of Mathematics, Bangabandhu Sheikh Mujibur Rahman Science & Technology University, Gopalganj-8100, BANGLADESH

³ Department of Mathematics, Islamic University, Kushtia-7003, BANGLADESH

Authors' contributions

This work was carried out in collaboration of all authors. Moreover the funding, computational suggestions, proof reading was also done by all authors and approved the final manuscript.

ABSTRACT

Magnetohydrodynamic mixed convection boundary layer flow of a nanofluid near the stagnation-point on a vertical plate with heat generation is investigated for both assisting and opposing flows are well thought-out. Different types of nanoparticles as copper (Cu), alumina (Al₂O₃) and titania (TiO₂) considering here. Using similarity approach the system of partial differential equations is transformed into ordinary differential equations which strongly depend on the magnetic parameter (M), buoyancy parameter (λ), Prandtl number (P_r), heat generation parameter (Q) and volume fraction parameter (ϕ). The coupled differential equations are numerically simulated using the Nactsheim-Swigert shooting technique together with Runge-Kutta six order iteration schemes. The velocity and temperature profiles are discussed and presented graphically. The comparison for dimensionless skin friction coefficient and local Nusselt number with previously published literature also take into account for the accuracy of the present analysis.

Keywords: MHD, mixed convection, nanofluid, Heat generation, stagnation-point flow

1. INTRODUCTION

Magneto-fluid-dynamics or hydro-magnetics is a limitless field of research which analyzed the study of the dynamics of electrically conducting fluids includes plasmas, liquid metals, and salt water or electrolytes etc. The expression magneto-hydrodynamics (MHD) is consists of three belongings such as magneto (magnetic field), hydro (liquid) and dynamics

*Corresponding author: Tel.: +61 04 70776627;

E-mail address: mdshakhaoath.khan@uon.edu.au , shakhaoathmathku@yahoo.com.

37 (movement of particles). As a consequence magnetic fields induce current flows in a
 38 dynamic fluid and create forces on the fluid and also adjust the magnetic field itself. The
 39 combination of the Navier-Stokes equations of fluid-mechanics and Maxwell's equations of
 40 electromagnetism consequently established MHD relations. Due to wide applications in heat
 41 exchangers, post accidental heat removal in nuclear reactors, geothermal and oil recovery,
 42 solar collectors, drying processes, building construction, etc. the Buoyancy flow [1] and heat
 43 transfer is a significant phenomenon in engineering systems.

44
 45 To incorporate the importance regarding MHD there is some suitable references
 46 from the literature [2-5], that reports MHD Flow of Oldroyd-B Fluid, Maxwell Fluid, Jeffrey
 47 Fluid also carried out MHD slip flow analysis of non-Newtonian fluid over a shrinking
 48 surface.

49
 50 Also as conventional heat transfer fluids, including oil, water, and ethylene glycol
 51 mixture are poor heat transfer fluids, since the thermal conductivity of these fluids plays
 52 important role on the heat transfer co-efficient between the heat transfer medium and the
 53 heat transfer surface.

54
 55 The effects of heat generation arise in high temperature ingredients processing
 56 operations also it can affect on heat transfer over an extending surface [6]. Choi [7] was the
 57 first who employ a technique to improve heat transfer is by using nano-scale particles in the
 58 base fluid and introduced the term of nanofluids as a novel class of fluid. As a result this type
 59 of fluids determines high thermal conductivity, significant change in properties such as
 60 viscosity and specific heat in comparison to the base fluid. Shehzad et al. [8-10] investigated
 61 on the boundary layer flow of thermal conductivity and heat generation/absorption, power
 62 law heat flux, heat source an thermal radiation. The heat transfer and fluid flow due to
 63 buoyancy forces in a partially heated enclosure using different types of nanoparticles is
 64 carried out by Oztop and Abu-Nada [11]. They have also provided the thermo physical
 65 properties of the fluid and nanoparticles as shown in Table. 1. Goodarzi et al. [12] also
 66 carried out the mixed convective laminar and turbulent nanofluid in a shallow rectangular
 67 enclosure by using a two-phase mixture model.

68
 69 **Table 1: Thermophysical possessions of the fluid and the nanoparticles [11, 12].**

70

Physical properties	Fluid phase (water)	Cu	Al ₂ O ₃	TiO ₂
$C_p(\text{J/kgK})$	4179	385	765	686.2
$\rho(\text{kg /m}^3)$	997.1	8933	3970	4250
$k(\text{W/mK})$	0.613	400	40	8.9538
$\alpha \times 10^{-7} (\text{m}^2/\text{s})$	1.47	1163.1	131.7	30.7
$\beta \times 10^{-7} (\text{m}^2/\text{s})$	21	1.67	0.85	0.9

71
 72
 73 Nanofluid-technology is now largely used in engineering and industrial applications. Due
 74 to this applications in recent years many researchers investigates some numerical and
 75 experimental analysis on nanofluids include convective instability [13] thermal conductivity
 76 [14, 15] and natural convective boundary-layer flow [16, 17]. Recently boundary layer heat-
 77 mass transfer free convection flows also in porous media of a nanofluid past a stretched
 78 sheet reported by Khan and Pop [18]. Hamad and Pop [19] studied MHD free convection
 79 rotating flow of a nanofluid. The boundary layer nanofluid flow with MHD radiative
 80 possessions recently predicted Md. Shakhaoath Khan et al. [20] analyzed. Khan and Pop

81 [21] analyzed boundary layer heat and mass transfer analysis past a wedge moving in a
 82 nanofluid. Very recently Tamim *et al.*[22] investigates the mixed convection boundary layer
 83 flow of a nanofluid near the stagnation-point on a vertical plate where the mixed convection
 84 flows are characterized by the buoyancy parameter λ , whereas for assisting flow, $\lambda > 0$ and
 85 for opposing flow $\lambda < 0$. Thesame problem corresponds to forced convection flow when the
 86 buoyancy effects are negligible ($\lambda = 0$).

87
 88 Recently there have been relatively few studies [23-32] that reports MHD boundary layer
 89 fluid as well as nanofluid flow as well.

90
 91 The present study predicting the MHD mixed convection boundary layer flow of a
 92 nanofluid near the stagnation-point on a vertical plate with heat generation for both assisting
 93 and opposing flows. And this work extended the study of Tamim *et al.*[22]. The governing
 94 equations are transformed into nonlinear ordinary differential equations which depend on the
 95 Magnetic parameter (M), buoyancy parameter (λ), Prandtl number (P_r), Heat generation
 96 parameter (Q) and volume fraction parameter (ϕ).The obtained nonlinear coupled ordinary
 97 differential equations are solved numerically using Nactsheim-Swigert [33] shooting iteration
 98 technique together with Runge-Kutta six order iteration schemes. The velocity and
 99 temperature distributions are discussed and presented graphically. The comparison for
 100 dimensionless skin friction coefficient and local Nusselt number with Tamim *et al.*[22] also
 101 take into account for the accuracy of the present analysis.

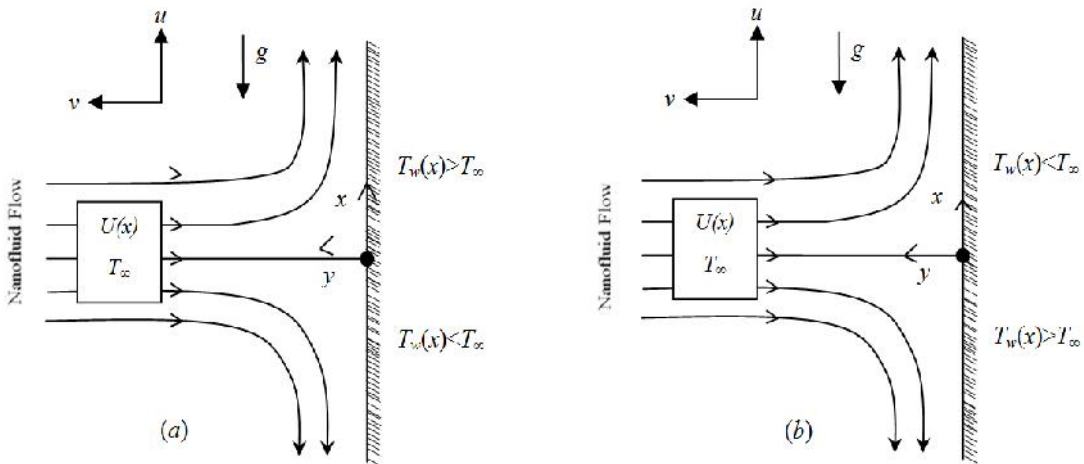
102
 103

104 2. FORMULATION OF THE PROBLEM

105

106 The steady two dimensional boundary layer mixed convection flow considered near the
 107 stagnation-point on a vertical flat plate. The physical configuration of this problem is shown
 108 in Fig. 1 [22]. No slip conditions occurs between the thermally equilibrium nanoparticles.
 109 Here the coordinate's x-axis is extending along the surface whereas the y-axis is measured
 110 normal to the surface.

111



112

113

113 **Fig. 1. Physical configuration and coordinates system**

114

115 The outer boundary layer of the x-component velocity taken as $U(x) = ax$ where a is positive
 116 constants and the plate temperature taken as proportional to the distance from the

117 stagnation-point, $T_w(x)=T_\infty+bx$, whereas $b>0$ indicates assisting flow which occurs when the
 118 superior part of the plate is heated while the lower half of the plate is cooled. And $b<0$
 119 indicates opposing flow which occurs if the superior part of the plate is cooled while the
 120 lower part of the plate is heated. Thus the buoyancy force arises here to assist the main flow
 121 field.

122

123 The governing equations for the laminar two-dimensional boundary layer heat
 124 transfer flow can be written as follows;

125
$$\frac{\partial u}{\partial x} + \frac{\partial v}{\partial y} = 0, \quad (1)$$

126
$$u \frac{\partial u}{\partial x} + v \frac{\partial u}{\partial y} = U \frac{dU}{dx} + \frac{\mu_{nf}}{\rho_{nf}} \left(\frac{\partial^2 u}{\partial y^2} \right) + \frac{[\varphi \rho_s \beta_s + (1-\varphi) \rho_f \beta_f] g (T - T_\infty) + \sigma B_0^2 (U - u)}{\rho_{nf}}, \quad (2)$$

127
$$u \frac{\partial T}{\partial x} + v \frac{\partial T}{\partial y} = \alpha_{nf} \frac{\partial^2 T}{\partial y^2} + \frac{Q_\infty}{\rho_f C_p} (T - T_\infty), \quad (3)$$

128

129 here, μ_{nf} is the viscosity of the nanofluid, α_{nf} is the thermal diffusivity of the nanofluid and ρ_{nf}
 130 is the density of the nanofluid, β_f and β_s are the thermal expansion coefficients of the base
 131 fluid and nanoparticle, respectively. The values of μ_{nf} , α_{nf} and ρ_{nf} can be written as;

132

133
$$\mu_{nf} = \frac{\mu_f}{(1-\varphi)^{2.5}}, \rho_{nf} = (1-\varphi)\rho_f + \varphi\rho_s, (\rho C_p)_{nf} = (1-\varphi)(\rho C_p)_f + \varphi(\rho C_p)_s, \quad (4)$$

134
$$\alpha_{nf} = \frac{k_{nf}}{(\rho C_p)_{nf}}, k_{nf} = \frac{(k_s + 2k_f) - 2\varphi(k_f - k_s)}{(k_s + 2k_f) + \varphi(k_f - k_s)},$$

134

135 where, ρ_f and ρ_s is density of the base fluid and nanoparticle respectively, μ_f is viscosity of the
 136 base fluid, k_f and k_s is the thermal conductivity of the base fluid and nanoparticle respectively
 137 and k_{nf} is the effective thermal conductivity of the nanofluid approximated by the Maxwell-
 138 Garnett model [11].

139

140 The boundary condition for the model is;

141
$$u = 0, v = 0, T = T_w(x) = T_\infty + bx \text{ at } y = 0,$$

142
$$u = U(x) = ax, T \rightarrow T_\infty \text{ as } y \rightarrow \infty. \quad (5)$$

143

144

145 3. SOLUTION OF THE FLOW FIELD

146

147

148 In order to conquer a similarity solution to eqs. (1) to (3) with the boundary
 149 conditions (5) the following dimensionless variables are used;

150
$$\eta = y \sqrt{\frac{a}{\nu_f}}, \psi = x \sqrt{a \nu_f} f(\eta), \theta = \theta(\eta) = \frac{T - T_\infty}{T_w - T_\infty} \text{ and } u = \frac{\partial \psi}{\partial y}, v = -\frac{\partial \psi}{\partial x}. \quad (6)$$

151

152 From the above transformations the non-dimensional, nonlinear, coupled ordinary differential
 153 equations are obtained as;

154

$$155 \quad f''' + (1-\varphi)^{2.5} (1-\varphi + \varphi\rho_s / \rho_p) [ff'' - f'^2 + 1 + \lambda\theta + M(1-f')] = 0, \quad (7)$$

$$156 \quad \theta'' + \left(P_r \frac{(1-\varphi) + \varphi(\rho C_p)_s / (\rho C_p)_f}{k_{nf} / k_f} \right) (f\theta' - f'\theta + Q\theta) = 0. \quad (8)$$

157

158 The transformed boundary conditions are as follows:

159

$$160 \quad \left. \begin{aligned} f = 0, f' = 0, \theta = 1 & \quad \text{at } \eta = 0 \\ f' = 1, \theta = 0 & \quad \text{as } \eta \rightarrow \infty. \end{aligned} \right\} \quad (9)$$

161

162 where the notation primes denote differentiation with respect to η and the parameters are
163 defined as;

164

$$165 \quad M = \frac{\sigma B_0^2}{\rho a}, \text{ Magnetic parameter}$$

$$166 \quad \lambda = \frac{G_r}{\text{Re}_x^2} = \frac{b[\varphi\rho_s\beta_s + (1-\varphi)\rho_f\beta_f]g}{\rho_{nf}a^2}, \text{ Buoyancy/thermal convection parameter}$$

$$167 \quad G_r = \frac{x^3[\varphi\rho_s\beta_s + (1-\varphi)\rho_f\beta_f]g(T_w - T_\infty)}{\rho_{nf}V_{nf}^2}, \text{ local Grashof number}$$

$$168 \quad \text{Re}_x = \frac{xU(x)}{V_{nf}}, \text{ local Reynolds number}$$

$$169 \quad P_r = \frac{\nu_f}{\alpha_f} \text{ Prandtl number and}$$

$$170 \quad Q = \frac{Q_\infty}{a\rho C_p}, \text{ heat source parameter}$$

171

172 The physical quantities of interest are the skin friction coefficient and the local Nusselt
173 number can be obtained [22] as follows;

174

$$175 \quad C_f [\text{Re}_x]^{1/2} = 2 \frac{f''(0)}{(1-\varphi)^{2.5}}, \quad (10)$$

$$Nu_x [\text{Re}_x]^{-1/2} = -\frac{k_{nf}\theta'(0)}{k_f}.$$

176

177 4. NUMERICAL SIMULATION

178 The non-dimensional, nonlinear, coupled ordinary differential eqs. (7) and (8) with boundary
179 conditions (9) are solved numerically using the Nactsheim and Swigert [33] shooting iteration
180 technique together with a sixth-order Runge-Kutta iteration scheme to determine the

181 continuity, momentum and energy as a function of the independent variable, η . In this
182 approach, the missing (unspecified) initial condition at the initial point of the interval is
183 assumed and the differential equation is integrated numerically as an initial value problem to
184 the terminal point. The accuracy of the assumed missing initial condition is then verified via
185 comparison with the computed value of the dependent variable at the terminal point with its
186 given value there. If a difference exists, another value of the missing initial condition must be
187 assumed and the process is repeated. This process is continued until the agreement
188 between the calculated and the given condition at the terminal point is within the specified
189 degree of accuracy. Extension of the iteration shell to considered system of differential eqns.
190 is straightforward; there are two asymptotic boundary condition and hence two unknown
191 surface conditions $f'(0)$ and $\theta(0)$.

192

193 **5. RESULTS AND DISCUSSION**

194

195 The numerical values of velocity and temperature have been computed for the magnetic
196 parameter, M , Thermal convective parameter, λ , Prandtl number, P_r , heat generation
197 parameter, Q , and volume fraction parameter, φ respectively. Among the parameters $\lambda > 0$
198 for assisting flows, $\lambda < 0$ for opposing flows and $\lambda = 0$ corresponding to forced convection
199 when the buoyancy force is absent. Different nanofluid-particles as copper (Cu), alumina
200 (Al_2O_3) and titania (TiO_2) are taken into account. To assess the accuracy of the numerical
201 results the Skin friction coefficient and surface heat rate compared with previous literature
202 [22] and shown in Table 2-4. And excellent agreement is observed from this comparison.
203 Also a consequence has been found that the skin friction coefficient and local Nusselt
204 number increase with increasing λ & φ .

205

206

207

208

209

210

211

212

213

214

Table 2: Comparison of the skin friction coefficient and the Nusselt number when $\lambda = 1$, $M=0$, and $Q=0$.

Nanoparticle	ϕ	$\lambda=1$ (Assisting flow)			
		Tamim <i>et al.</i> [22]	Present Results	Tamim <i>et al.</i> [22]	Present Results
		$[Re_x]^{1/2} C_f$	$[Re_x]^{1/2} C_f$	$[Re_x]^{1/2} Nu_x$	$[Re_x]^{1/2} Nu_x$
Cu	0.00	3.05355	3.05687	1.65242	1.66482
	0.05	3.91833	3.91987	1.87279	1.89754
	0.10	4.81536	4.81754	2.08336	2.08458
	0.15	5.77580	5.79630	2.29008	2.29145
	0.20	6.82739	6.84644	2.49642	2.49783
Al ₂ O ₃	0.00	3.05355	3.05683	1.65242	1.66092
	0.05	3.51805	3.52584	1.80652	1.81547
	0.10	4.02763	4.02359	1.96055	1.97580
	0.15	4.59295	4.59578	2.11528	2.12254
	0.20	5.22693	5.22699	2.27145	2.28654
TiO ₂	0.00	3.05355	3.05482	1.65242	1.66874
	0.05	3.53844	3.53963	1.78590	1.79872
	0.10	4.06820	4.06899	1.91667	1.92547
	0.15	4.65406	4.65546	2.04529	2.04689
	0.20	5.30940	5.31205	2.17213	2.17321

215
216
217
218
219

Table3: Comparison of the skin friction coefficient and the Nusselt number when $\lambda = 0$, $M=0$, and $Q=0$.

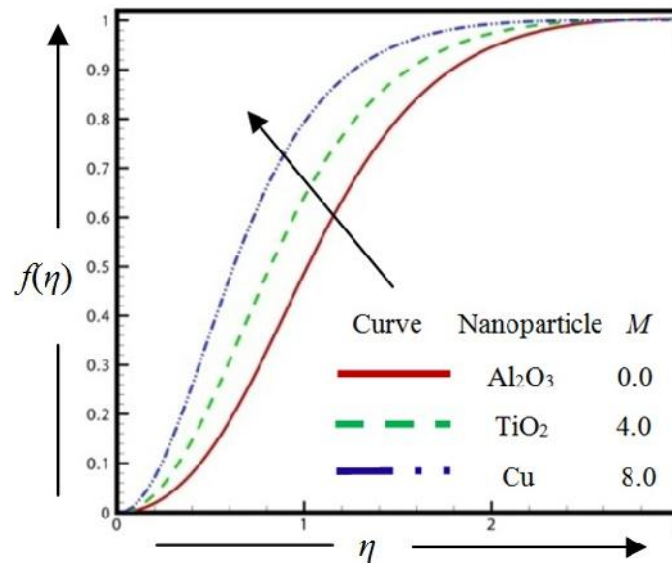
Nanoparticle	ϕ	$\lambda = 0$ (Forced convection)			
		Tamim <i>et al.</i> [22]	Present Results	Tamim <i>et al.</i> [22]	Present Results
		$[Re_x]^{1/2} C_f$	$[Re_x]^{1/2} C_f$	$[Re_x]^{1/2} Nu_x$	$[Re_x]^{1/2} Nu_x$
Cu	0.00	2.46518	2.47584	1.57343	1.58741
	0.05	3.10770	3.11459	1.77577	1.78421
	0.10	3.76865	3.78452	1.96921	1.97710
	0.15	4.47381	4.49874	2.15931	2.16879
	0.20	5.24549	5.25568	2.34936	2.35510
Al ₂ O ₃	0.00	2.46518	2.47412	1.57343	1.58741
	0.05	2.81753	2.82568	1.71690	1.72201
	0.10	3.20411	3.21254	1.86033	1.87405
	0.15	3.63365	3.64582	2.00450	2.01373
	0.20	4.11665	4.12658	2.15020	2.16687
TiO ₂	0.00	2.46518	2.47178	1.57343	1.58957
	0.05	2.83469	2.84581	1.69742	1.69987
	0.10	3.23858	3.24410	1.81898	1.82574
	0.15	3.68615	3.69870	1.93870	1.94783
	0.20	4.18844	4.19973	2.05698	2.06547

220
221
222

Table 4: Comparison of the skin friction coefficient and the Nusselt number when $\lambda = -1$, $M=0$, and $Q=0$.

Nanoparticle	ϕ	$\lambda = -1$ (Opposing flow)			
		Tamim et al.[22]	Present Results	Tamim et al.[22]	Present Results
		$[Re_x]^{1/2} C_f$	$[Re_x]^{1/2} C_f$	$[Re_x]^{1/2} Nu_x$	$[Re_x]^{1/2} Nu_x$
Cu	0.00	1.82621	1.83584	1.47787	1.48741
	0.05	2.22075	2.23257	1.65618	1.66254
	0.10	2.61683	2.62250	1.82647	1.83102
	0.15	3.03459	3.05471	1.99394	1.99871
	0.20	3.49056	3.49910	2.16169	2.18457
Al ₂ O ₃	0.00	1.82621	1.83258	1.47787	1.49542
	0.05	2.05421	2.07582	1.60756	1.61287
	0.10	2.30424	2.30871	1.73719	1.74410
	0.15	2.58292	2.59651	1.86760	1.87412
	0.20	2.89819	2.89993	1.99963	2.00478
TiO ₂	0.00	1.82621	1.83247	1.47787	1.48974
	0.05	2.06795	2.07412	1.58950	1.59952
	0.10	2.33229	2.34127	1.69904	1.71243
	0.15	2.62650	2.63658	1.80712	1.81470
	0.20	2.95913	2.96524	1.91423	1.92105

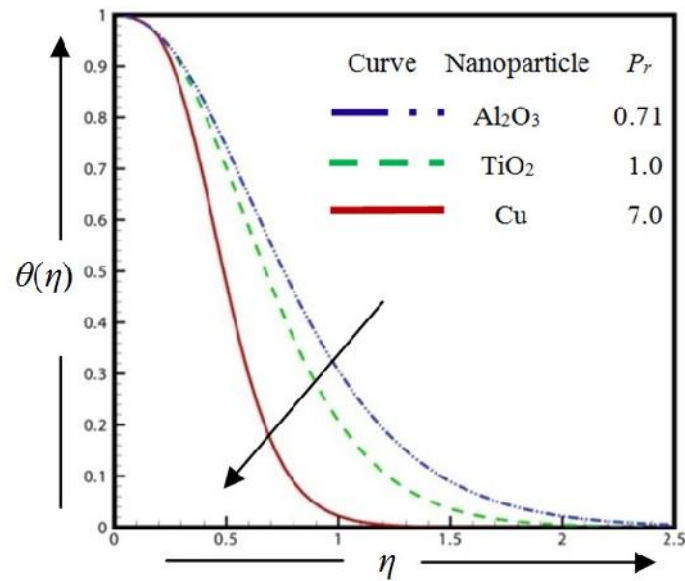
223
224



225
226
227
228

Fig. 2. Velocity distribution for different types of nanoparticle and M where $\phi=0.3$, $\lambda =2.0$, $P_r=0.71$ & $Q=1.0$

229 Fig. 2 depicts the velocity profiles for different values of nanoparticles and magnetic
230 parameter, M when $\lambda = 2$ (assisting flow). As a result, the momentum boundary layer
231 thickness increases. It is evident from these figures that velocity profiles satisfy the far field
232 boundary conditions asymptotically and validated the numerical results.



234

235

236

237

Fig. 3. Temperature distribution for different types of nanoparticle and P_r , where $\phi=0.3$, $\lambda=2.0$, $Q=1.0$ & $M=4.0$.

238

239

240

Fig. 3 represents the temperature profiles for different values of nanoparticles and Prandtl number P_r , when $\lambda = 2$ (assisting flow). It was found the temperature boundary layer decreases as Prandtl number increases.

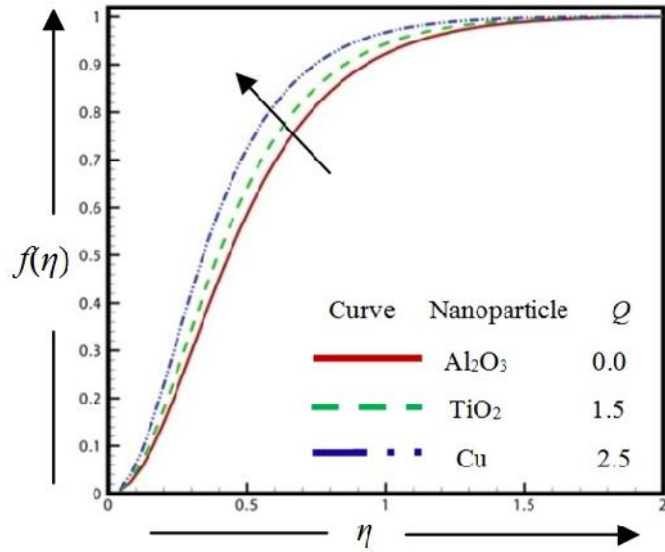
241

242

243

244

The effect of the heat generation and different nanoparticle on velocity and temperature distributions in the case of $\lambda = 0$ (forced convection) are illustrated in Fig. 4 and 5, respectively. It is observed that the momentum boundary layer thickness increases while the thermal boundary layer decreases as the heat generation grows.



245

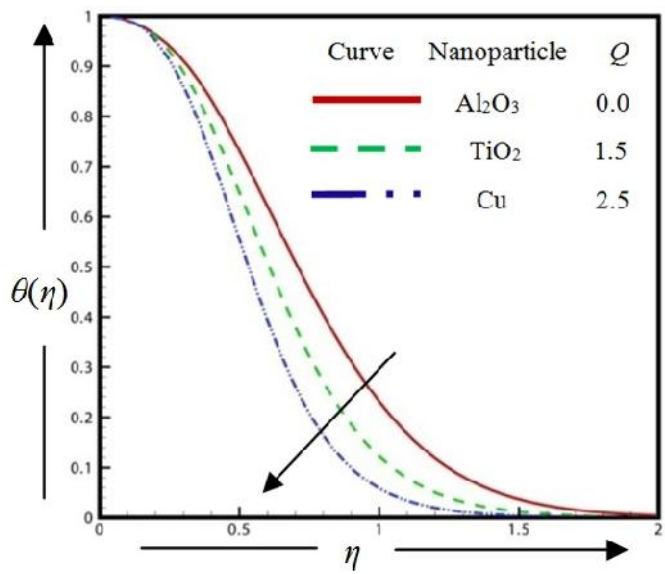
246

247

248

249

Fig. 4. Velocity distribution for different types of nanoparticle and Q where $\varphi=0.3$, $\lambda=0.0$, $P_r=0.71$ & $M=4.0$.



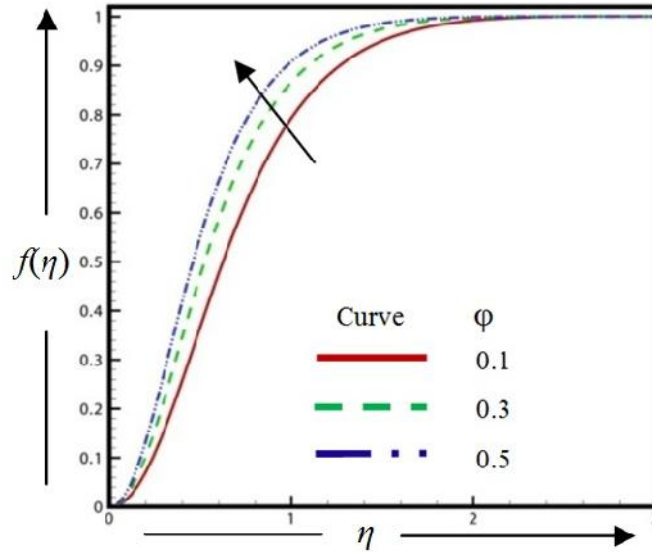
250

251

252

253

Fig. 5. Temperature distribution for different types of nanoparticle and Q where $\varphi=0.3$, $\lambda=0.0$, $P_r=0.71$ & $M=4.0$.



254

Fig. 6. Velocity distribution for different types of volume fraction parameter, ϕ where $Q=1.0$, $\lambda = -2.0$, $P_r=0.71$ & $M=4.0$.

255

256

257

258

259

260

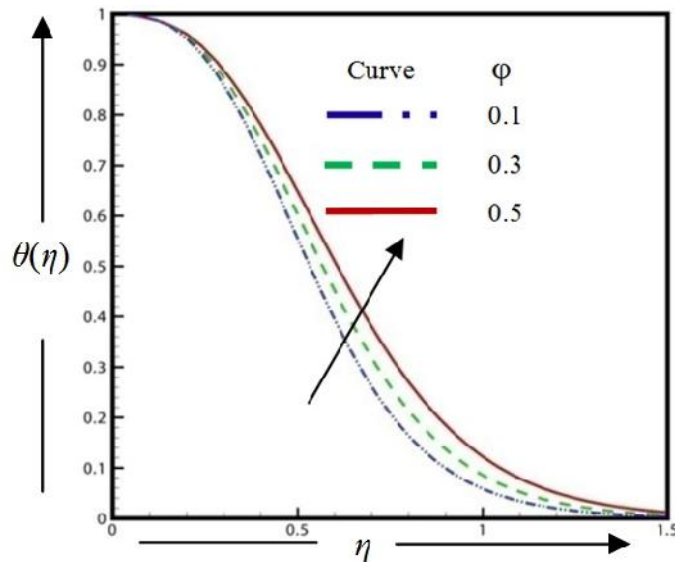
261

262

263

264

Fig. 6 show the velocity profiles for various values of the volume fraction parameter ϕ in the case of titania (TiO_2)-water when $\lambda = -2$ (opposing flow). It is noted that due to the fact that the presence of nano-solid-particles leads to further diminishing of the boundary layer the momentum boundary layer thickness increases with the volume fraction parameter.



265

Fig. 7. Temperature distribution for different types of volume fraction parameter, ϕ where $Q=1.0$, $\lambda = -2.0$, $P_r=0.71$ & $M=4.0$.

266

267

268

269 Figure 7 is presented to show the effect of the TiO_2 nanoparticle volume fraction on
270 temperature distribution. From this figure, when the volume of TiO_2 nanoparticles increases,
271 the thermal conductivity increases, and then the thermal boundary layer thickness increases
272 progressively.

273

274 **6. CONCLUDING REMARKS**

275

276 Magnetohydrodynamics mixed convection boundary layer heat transfer flow of a nanofluid near
277 the stagnation-point on a vertical plate with the effect of heat generation has been studied.
278 Heat transfer characteristics of copper (Cu), alumina (Al_2O_3) and titania (TiO_2) nanoparticles is
279 observed. The momentum boundary layer thickness increases for all cases. The temperature
280 boundary layer thickness is going down for varying different types of nanoparticle, increasing
281 heat generation and Prandtl number respectively. But at higher volume fraction parameter the
282 temperature boundary layer thickness rises gradually. The current study has applications in
283 high-temperature nano-technological materials processing.

284

285 **7. NOMENCLATURE**

286

287 a, b constant

288 Al_2O_3 alumina

289 B_0 magnetic induction

290 C_f Skin friction coefficient

291 C_p specific heat at constant pressure

292 Cu copper

293 G_r Grashof number

294 k thermal conductivity

295 M magnetic parameter

296 Nu_x Local Nusselt number

297 P fluid pressure

298 P_r Prandtl number

299 Q heat source parameter

300 Q_0 heat generation constant

301 Re_x Local Reynolds number

302 T temperature at the surface

303 T_∞ ambient temperature as $y \rightarrow \infty$

304 TiO_2 titania

305 u, v velocity components along x, y axes respectively

306 $U(x)$ free stream velocity

307 **Greek symbols**

308 ν kinematic viscosity

309 ρ density

310 σ conductivity of the material

311 α thermal diffusivity

312 β co-efficient of thermal expansion

313 λ Buoyancy/thermal convection parameter

314 μ dynamic viscosity

315 η similarity variable

316 τ_w Wall shear stress

317 ψ stream function

318 φ volume fraction parameter

319 $f'(\eta)$ dimensionless velocity

320 $\theta(\eta)$ dimensionless temperature

321

322

323

324 **8. ACKNOWLEDGEMENTS**

325 The authors are very thankful to the editor and reviewers for their constructive comments
326 and valuable suggestions to improve this research paper.

327 **9. COMPETING INTERESTS**

328

329 The authors declare that they have no competing interests.

330

331

332 **10. REFERENCES**

333

334

335 1. Ostrach S. Natural convection in enclosures. *J. Heat Transfer*. 1988; 110: 1175–1190.

336 2. Hayat T, Shehzady SA, Mustafaz M and Hendi A. MHD Flow of an Oldroyd-B Fluid
337 through a Porous Channel. *International Journal of Chemical Reactor Engineering*.
338 2012; 10: A8.

339

340 3. Shehzad SA, Ahmad A and Hayat T. Hydromagnetic Steady Flow of Maxwell Fluid over
341 a Bidirectional Stretching Surface with Prescribed Surface Temperature and Prescribed
342 Surface Heat Flux. *Plos One*. 2013; 8: e68139.

343

- 344 4. Shehzad SA, Alsaedi A and Hayat T. Influence of Thermophoresis and Joule Heating on
345 The Radiative Flow of Jeffrey Fluid With Mixed Convection. *Brazilian Journal of*
346 *Chemical Engineering*. 2013; 30: 897-908.
347
- 348 5. Turkyilmazoglu M. Dual and triple solutions for MHD slip flow of non-Newtonian fluid
349 over a shrinking surface. *Comput. Fluids*. 2012; 70: 53-58.
350
- 351 6. Vajravelu K and Hadjinicalaou A. Heat transfer in a viscous fluid over a stretching sheet
352 with viscous dissipation and internal heat generation. *Int. Comm. Heat Mass Trans.*
353 1993; 20: 417-430.
- 354 7. Choi SUS. Enhancing Thermal Conductivity of Fluids With Nanoparticles, Development
355 and Applications of Non- Newtonian Flows. D.A. Siginer and H. P. Wang, eds., ASME
356 MD- vol. 231 and FED-vol. 66, USDOE, Washington, DC (United States), 1995;99-105.
357
- 358 8. Shehzad SA, Alsaedi A, Hayat T and Alhuthali MS. Three-Dimensional Flow of an
359 Oldroyd-B Fluid with Variable Thermal Conductivity and Heat Generation/Absorption.
360 *Plos One*. 2013; 8: e78240.
361
- 362 9. Shehzad SA, Qasim M, Hayat T, Sajid M, Obaidat S. Boundary layer flow of Maxwell
363 fluid with power law heat flux and heat source. *International Journal of Numerical*
364 *Methods for Heat & Fluid Flow*. 2013; 23(7): 1225 – 1241.
365
- 366 10. Shehzad SA. MHD mixed convection flow of thixotropic fluid with thermal radiation. *Heat*
367 *Transfer Research*. 2013; 44: 687-702.
- 368 11. Oztop HF and Abu-Nada E. Numerical study of natural convection in partially heated
369 rectangular enclosures filled with nanofluids. *International Journal of Heat and Fluid*
370 *Flow*. 2008; 29: 1326–1336.
- 371 12. Goodarzi M, Safaei MR, Ahmadi G, Vafai K, Dahari M, Jomhari N and Kazi SN. An
372 Investigation of Laminar and Turbulent Nanofluid Mixed Convection in a Shallow
373 Rectangular Enclosure Using a Two-phase Mixture Model. *International Journal of*
374 *Thermal Sciences*. 2014; 75: 204-220.
- 375 13. Kang Ki JYT and Choi CK. Analysis of convective instability and heat transfer
376 characteristics of nanofluids. *Phys. Fluids*. 2004;16: 2395-2401.
- 377 14. Kang HU, Kim SH and Oh JM. Estimation of thermal conductivity of nanofluid using
378 experimental effective particle volume. *Exp. Heat Transfer*. 2006;19: 181-191.
- 379 15. Jang SP, Choi SUS. Effects of various parameters on nanofluid thermal conductivity.
380 *ASME J. Heat Transfer*. 2007;129: 617-623.
- 381 16. Nield A and Kuznetsov AV. The Cheng–Minkowycz problem for natural convective
382 boundary-layer flow in a porous medium saturated by a nanofluid. *Int. J. Heat and Mass*
383 *Transfer*. 2009; 52: 792 – 5795.
- 384 17. Kuznetsov AV and Nield DA. Natural convective boundary-layer flow of a nanofluid past
385 a vertical plate. *Int. J. of Thermal Sci*. 2010; 49: 243 -247.

- 386 18. Khan WA and Pop I. Free convection boundary layer flow past a horizontal flat plate
387 embedded in a porous medium filled with a nanofluid. *ASME J. Heat Transfer*. 2011;
388 133: 157-163.
- 389 19. Hamad MAA and Pop I. Unsteady MHD free convection flow past a vertical permeable
390 flat plate in a rotating frame of reference with constant heat surface in a nanofluid. *Heat*
391 *Mass Transfer*. 2012; 47: 1517-1524.
- 392 20. Khan MS, Alam MM and Ferdows M. Effects of Magnetic field on Radiative flow of a
393 Nanofluid past a Stretching Sheet. *Procedia Engineering Elsevier*. 2013; 56: 316-322.
- 394 21. Khan WA and Pop I. Boundary Layer Flow Past a Wedge Moving in a Nanofluid.
395 *Mathematical Problems in Engineering*, 2013: 1-7.
- 396 22. Tamim H., Dinarvand PPS, Hosseini PPR, Khalili PS and Khalili PA. Mixed Convection
397 Boundary-layer Flow of a Nanofluid Near Stagnation-point on a Vertical Plate with
398 Effects of Buoyancy Assisting and Opposing Flows. *Research Journal of Applied*
399 *Sciences, Engineering and Technology*. 2013; 6: 1785-1793.
- 400 23. Khan MS, Alam MM and Ferdows M. Finite Difference Solution of MHD Radiative
401 Boundary Layer Flow of a Nanofluid past a Stretching Sheet. Proceeding of the
402 International Conference of Mechanical Engineering 2011 (ICME-11), FL-011, BUET,
403 Dhaka, Bangladesh.
- 404 24. Khan MS, Alam MM and Ferdows M. MHD Radiative Boundary Layer Flow of a
405 Nanofluid past a Stretching Sheet. Proceeding of the International Conference of
406 Mechanical Engineering and Renewable Energy 2011 (ICMERE-11), PI-105,
407 CUET, Chittagong, Bangladesh.
- 408 25. Khan MS, Karim Ifsana, Ali LE and Islam A. MHD Free Convection Boundary layer
409 Unsteady Flow of a Nanofluid along a stretching sheet with thermal Radiation and
410 Viscous Dissipation Effects. *International Nano Letters*, 2012; 2:24.
- 411 26. Ferdows M, Khan, MS, Alam MM and Sun S. MHD Mixed convective boundary layer flow
412 of a nanofluid through a porous medium due to an Exponentially Stretching sheet.
413 *Mathematical problems in Engineering*. 2012; 3: 2551-1557.
- 414 27. Khan M.S., Wahiduzzaman M, Sazad M.A.K and Uddin M.S. Finite difference solution of
415 MHD free convection heat and mass transfer flow of a nanofluid along a Stretching
416 sheet with Heat generation effects. *Indian Journal of Theoretical Physics*. 2012; 60: 285-
417 306.
- 418 28. Ferdows M, Khan MS, Alam M.M. and Bég OA. Numerical Study of Transient
419 Magnetohydrodynamic Radiative Free Convection Nanofluid Flow from a Stretching
420 Permeable Surface. *Journal of Process Mechanical Engineering*. 2013: 1-16.
- 421 29. Beg OA, Khan MS, Karim Ifsana, Ferdows M and Alam M.M. Explicit Numerical study of
422 Unsteady Hydromagnetic Mixed Convective Nanofluid flow from an Exponential
423 Stretching sheet in Porous media. *Applied Nanoscience*. October 2013.
- 424 30. Khan MS, Karim Ifsana and Biswas MHA. Heat Generation, Thermal Radiation and
425 Chemical Reaction Effects on MHD Mixed Convection Flow over an Unsteady Stretching

- 426 Permeable Surface. *International Journal of Basic and Applied Science*. 2012; 1(2): 363-
427 377.
428
- 429 31. Khan MS, Karim Ifsana and Biswas MHA. Non-Newtonian MHD Mixed Convective
430 Power-Law Fluid Flow over a Vertical Stretching Sheet with Thermal Radiation, Heat
431 Generation and Chemical Reaction Effects. *Academic Research International*. 2012;
432 3(3): 80-92.
433
- 434
- 435 32. Khan MS, Karim Ifsana and Islam MS. Possessions of Chemical Reaction on MHD Heat
436 and Mass Transfer Nanofluid Flow on a Continuously Moving Surface. *American
437 Chemical Science Journal*. 2014; 4(3): 401-415.
- 438 33. Nachtsheim PR and Swigert P. Satisfaction of the asymptotic boundary conditions in
439 numerical solution of the system of non-linear equations of boundary layer type. *NASA*,
440 1965; TND-3004.
- 441